Broadband Nonreciprocal THz Amplification in Luminal Graphene Metasurfaces

E. Galiffi[1], P. A. Huidobro[1,2], and J. B. Pendry[1]

[1] *Condensed Matter Theory Group, The Blackett Laboratory, Imperial College London, UK*
[2] *Instituto de Telecomunicações, Instituto Superior Tecnico-University of Lisbon, Portugal*
(Dated: July 22, 2019)

Time has emerged as a new degree of freedom for metamaterials, promising new pathways in wave control. However, electromagnetism suffers from limitations in the modulation speed of material parameters. Here we argue that these limitations can be circumvented by introducing a traveling-wave refractive index modulation, with the same phase velocity of the waves. We show how the concept of "luminal grating" can yield giant nonreciprocity, achieve efficient one-way amplification, pulse compression and frequency up-conversion, proposing a realistic implementation in double-layer graphene.

Temporal control of light is a long-standing dream, which has recently demonstrated its potential to revolutionize optical and microwave technology, as well as our understanding of electromagnetic theory, overcoming the stringent constraint of energy conservation [1]. Along with the ability of time-dependent systems to violate electromagnetic reciprocity [2–4], realising photonic isolators and circulators [5–8], amplify signals [9], perform harmonic generation [10, 11] and phase modulation [12], new concepts from topological [13–15] and non-Hermitian physics [16, 17] are steadily permeating this field.

However, current limitations to the possibility of significantly fast modulation in optics has constrained the concept of time-dependent electromagnetics to the radio frequency domain, where varactors can be used to modulate capacitance [18], and traveling-wave tubes are commonly used as (bulky) microwave amplifiers [19]. In the visible and near IR, optical nonlinearities have often been exploited to generate harmonics, and realize certain nonreciprocal effects [20]. However, nonlinearity is an inherently weak effect, and high field intensities are typically required.

In this Letter, we challenge the need for high modulation frequencies, demonstrating that strong and broadband nonreciprocal response can be obtained by complementing the temporal periodic modulation of an electromagnetic medium with a spatial one, in such a way that the resulting traveling-wave modulation profile appears to drift uniformly at the speed of the wave. Exploiting acoustic plasmons in double-layer graphene (DLG), we show that unidirectional amplification and compression can be realistically accomplished in such luminal gratings, despite the intrinsic limitations in the modulation speed of graphene. Our results hold potential for efficient THz generation, loss-compensation and amplification of plasmons, overcoming the typical trade-off between plasmon confinement and loss.

Bloch (Floquet) theory dictates that the wavevector (frequency) of a monochromatic wave propagating in a spatially (temporally) periodic medium can only Bragg-scatter onto a discrete set of harmonics, determined by the reciprocal lattice vectors. This still holds true when the modulation is of a travelling-wave type, whereby Bragg scattering couples Fourier modes which differ by a discrete value of both energy and momentum combined [2, 7, 21–24]. As shown in Fig. 1 for a 1D system, these space-time reciprocal lattice vectors can be defined to take any angle in phase space, depending on whether a generic traveling-wave modulation of the material parameters of the form $\delta\epsilon(gx - \Omega t)$ is spatial (panel a: $\Omega = 0$), temporal (d: $g = 0$), or spatiotemporal (b,c: $g \neq 0, \Omega \neq 0$). Given the slope c of the bands in a Brillouin diagram, which denotes the velocity of waves in a dispersionless medium, the speed of the traveling-wave modulation defines a subluminal regime $\frac{\Omega}{g} < c$ (a,b), whereby conventional vertical band gaps open [21], and a superluminal one $\frac{\Omega}{g} < c$ (c,d), characterized by horizontal, unstable k-gaps [22, 25]. A common example of the latter for $g = 0$ (Fig. 1d), is the parametric amplifier: when the parameters governing an oscillatory system are periodically driven at twice its natural frequency, exponential amplification occurs, as a result of the unstable k-gap at frequency $\omega = \Omega/2$.

The transition between the regimes in Figs. 1b and 1c is an exotic degenerate state, whereby all forward-propagating modes are uniformly coupled to each other, whereas the system is transparent to backward-traveling waves. Due to its broadband spectral degeneracy in the absence of dispersion, this system is highly unstable, thus preventing a meaningful definition of its band structure. Nevertheless, if we consider transmission through a spatially (temporally) finite system with well-defined boundary conditions, causality can be imposed in the unmodulated regions of space (time), and an expansion can be carried out in terms of eigenfunctions, as detailed in [26].

In luminal gratings, the photonic transitions induced by the modulation of the refractive index are no longer interband [27], but intraband, and can therefore be driven by means of any refractive index modulation, regardless of how adiabatic, whose reciprocal lattice vector (g, Ω) satisfies the speed matching condition $\Omega/g = c$. Hence, any limitation in modulation frequency Ω can be compensated, in principle, by a longer spatial period $L = 2\pi/g$. Notably, these can be locally induced by modulating the properties of the medium, and can thus synthetically move at any speed, including and exceeding the speed of light, in analogy with the touching point of a water wave
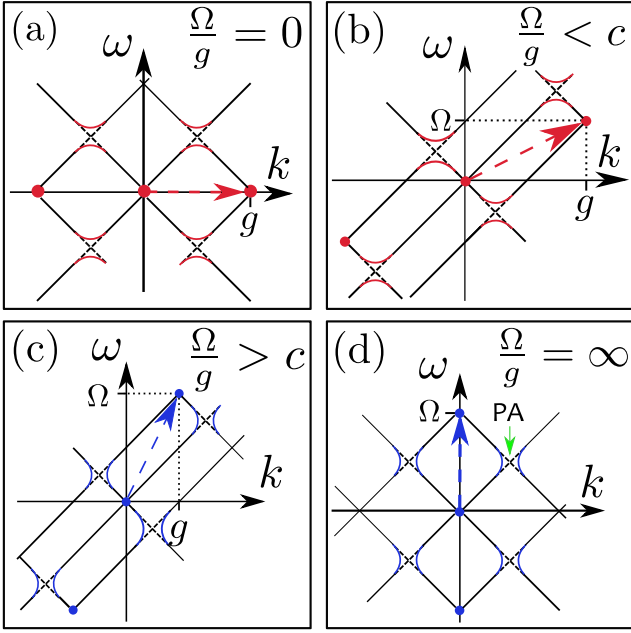
FIG. 1. (a) The band structure of a conventional spatial crystal is repeated in phase space at $k = ng$, $n \in \mathbb{Z}$, forming vertical band gaps (ω-gaps). (b) Similarly, the band structure of a traveling-wave-modulated crystal is symmetric under discrete translations by an oblique reciprocal lattice vector (g, Ω). When $\frac{\Omega}{g} < c$, ω-gaps open, whereas (c) $\frac{\Omega}{g} > c$ leads to unstable k-gaps. (d) Finally, if the wavelength of the modulation $L \to \infty$, then $g \to 0$, so that the system is effectively only modulated in time In this case, the modulation speed $\frac{\Omega}{g} \to \infty$ and the system becomes a conventional, reciprocal, parametric oscillator. The transition between (b) and (c), whereby the light-line and the reciprocal lattice vector are aligned, is a luminal grating.

front propagating almost perpendicularly to a beach, or the junction between the blades of a pair of scissors.

Due to their ease of manipulation, metasurfaces, the two-dimensional analogues of metamaterials, offer the most promising playground to realize dynamical effects [1, 28, 29], also due to the rise of tunable two-dimensional materials [30, 31]. Recently, graphene has emerged as a platform to enhance light-matter interactions [32–35], realizing atomically thin metasurfaces [12, 36–39]. Its doping level, which can be as high as ≈ 2 eV [40, 41], can be dynamically modulated, with reported response times of ≈ 2.2 ps, and relative modulations of 38% [42]. In addition, modern-quality graphene features extremely high electron mobility, with measured experimental values of $\sim 350'000$ cm^2/(V·s) [43]. Alternative schemes for the amplification of graphene plasmons have been proposed, such as the use of drift currents [44, 45], periodic doping modulation [46], adiabatic doping suppression [47], and plasmonic Čerenkov emission by hot carriers [48].

The typical dispersion relation of graphene plasmons

follows a square root behaviour $\omega \sim \sqrt{k}$, where ω is the angular frequency and k is the in-plane wavevector. However, in a double-layer configuration, a second "acoustic" plasmon branch arises, whose dispersion:

$$\omega \propto \sqrt{\epsilon_F}\sqrt{k(1 - e^{-\delta_0 k})} \simeq \sqrt{\delta_0 \epsilon_F}k(1 - \frac{\delta_0 k}{4}) \quad (1)$$

is linear in the limit of small interlayer gap $\delta_0 \ll k^{-1}$ [49].

An equivalent system has recently been realized with graphene near gold, which acts as a mirror, demonstrating nanoscale confinement of THz acoustic plasmons with surprisingly long lifetimes [50, 51]. Here we exploit the linearity of this acoustic plasmon band to realize a luminal metasurface.

We assume a semiclassical (Drude) conductivity model, which is accurate as long as $\hbar\omega \ll \epsilon_F$ and $k \ll k_F$, where $\epsilon_F = 1.5$ eV $\approx 2\pi\hbar \times 362$ THz is the Fermi energy, $k_F = \frac{\epsilon_F}{\hbar v_F} \approx 2.3$ rad/nm, is the Fermi wavevector and $v_F \approx 9.7 \times 10^5$ ms^{-1} is the Fermi velocity. Our setup consists of two graphene layers, whose Fermi levels are modulated as $\epsilon_F(x,t) = \epsilon_{F,0}[1 + 2\alpha\cos(gx - \Omega t)]$ (Fig. 2b, inset). Dispersion is accounted for, by expressing the constitutive relation for the current:

$$J(x,t) = e^{i(kx - \omega t)}\sum_n J_n e^{in(gx - \Omega t)} \quad (2)$$

in Fourier space, where the conductivity modulation couples neighbouring frequency harmonics:

$$J_n = \frac{e^2 \epsilon_{F,0}}{\pi\hbar^2}\frac{E_n + \alpha(E_{n+1} + E_{n-1})}{\gamma - i(\omega + n\Omega)}, \quad (3)$$

where E_n is the nth Fourier amplitude of the in-plane electric field, which is continuous at the layer positions $z = 0$ and $z = \delta_0$ [26]. The magnetic field of the p-polarized wave:

$$H_y(x,z,t) = e^{i(kx - \omega t)}\sum_n H_n e^{in(gx - \Omega t) + \kappa_n z} \quad z < 0 \quad (4)$$

is discontinuous at the layers by the surface current [49].

This system can be accurately described within an adiabatic regime, since the modulation frequency $\Omega \ll \omega$. Furthermore, since acoustic plasmons carry much larger momentum than photons, the modes are strongly quasistatic, so that the out of plane decay constant $\kappa_n \simeq k + ng$, and coupling to radiation is negligible, given that both the spatial and temporal frequencies of the grating are much smaller than the plasmon wavevector and frequency.

Plugging our ansatz into Maxwell's equations, and applying boundary conditions, we arrive at an eigenvalue equation for the plasmon frequencies ω. Taking advantage of the adiabatic assumption, we can solve the scattering problem in the time domain (Fig. 2c), as detailed in [26]. At times $t < 0$ the plasmon is propagating with
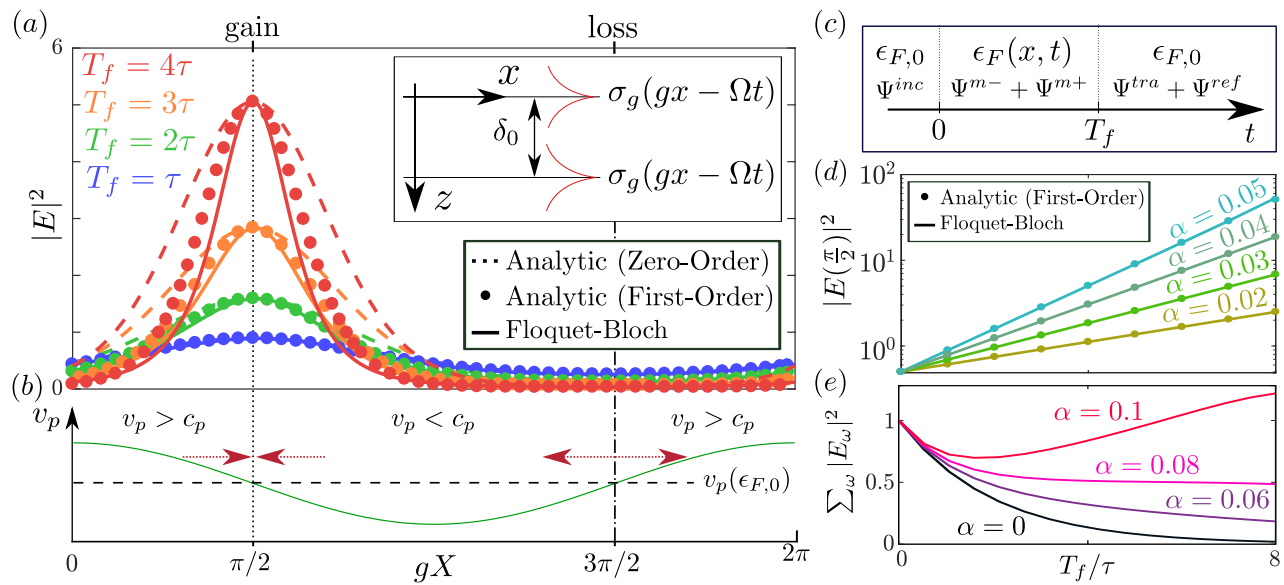
FIG. 2. (a) The plasmon instensity in modulated DLG (inset) is locally amplified and compressed, as a luminal modulation is applied over a time-window T_f. Continuous lines correspond to our Floquet-Bloch theory, whereas dotted lines and circles are obtained from our analytic model to zeroth and first order respectively. In (a) and (d) we use low loss to demonstrate the effect, corresponding to an electron scattering rate $\gamma = \frac{v_F^2 e}{m\epsilon_{F,0}}$, with a mobility $m = 10^6$ cm^2/(V·s). (b) The plasmon compresses at the gain-point $gx = \pi/2$, which acts as an attractor, towards which waves occupying the region $-\pi/2 < gx < \pi/2$ ($\pi/2 < gx < 3\pi/2$) advance (lag), due to the higher (lower) local phase velocity v_p. Conversely, the loss-point $3\pi/2$ is depleted of energy. (c) The scattering problem is most conveniently solved in the time domain: an incident wave is scattered into a transmitted and a time-reversed wave after the modulation has been applied over a time-window T_f. (d) The field intensity at the gain-point grows exponentially with both modulation time T_f and amplitude α, matching exactly our analytical model (dots). (e) The total power of the plasmon reduces initially, due to dissipation. Once the pulse is localised near the gain-point, loss compensation starts, and even amplification is possible by increasing the modulation strength α. In (e) we assume higher loss, $m = 10^5$ cm^2/(V·s), to show the realistic potential for loss-compensation and amplification.

frequency ω and wavevector k. As the doping modulation is switched on at $t = 0$, the system is periodic in space, so that its original quasi-momentum k is conserved. We can thus obtain the associated frequency eigenvalues, and propagate the solution up to time $t = T_f$, when it is switched off, and the pulse will consist of a forward-traveling wave, and a time-reversed one. The latter, however, is negligibly small, due to the strongly unidirectional character of the coupling, as confirmed by our calculations.

Fig. 2a demonstrates plasmon amplification and compression for different modulation times T_f. Here, we use a modulation amplitude $\alpha = 0.05$, interlayer gap $\delta_0 = 1$ nm and a modulation frequency $\Omega/2\pi = 1.2$ GHz, which corresponds to a modulation period $\tau = \Omega/2\pi \approx 8$ ps and length $2\pi/g \approx 26$ μm, and an input frequency $\omega/2\pi = 1$ THz. Parametrizing the modulation profile as $gX = gx - \Omega t$, there are two points where the long-wavelength phase velocity of the plasmon $v_p(X) = \lim_{k\to 0} \frac{\omega}{k} \propto \sqrt{\epsilon_{F,0} + 2\alpha\cos(gX)}$ is matched by the modulation speed $c_p = \frac{\Omega}{g}$, namely $gX = \pi/2$ and $gX = 3\pi/2$. As illustrated in Fig. 2b, those components of the plasmon which sit at $-\pi/2 < gX < \pi/2$ experience a higher Fermi level, and hence a higher phase velocity,

whereas those sitting at $\pi/2 < gX < 3\pi/2$ lag, so that the point $gX = \pi/2$ acts as an attractor, or gain-point, where the modulation imparts energy into the plasmon. Conversely, $gx = 3\pi/2$ is a repellor, or loss-point, where energy is absorbed by the modulation drive.

This effect can be modelled as follows: consider a non-dispersive medium where $\varepsilon(x,t) = 1 + 2\alpha\cos(gx - \Omega t)$, with $\Omega/g = c_0$. Following the derivation of Poynting's theorem, we can write:

$$\nabla \cdot (\mathbf{E} \times \mathbf{H}) = -\frac{\mu_0}{2}\frac{\partial H^2}{\partial t} - \frac{\varepsilon_0\varepsilon}{2}\frac{\partial E^2}{\partial t} - \varepsilon_0\frac{\partial \varepsilon}{\partial t}E^2, \quad (5)$$

so that the total time-derivative of the local energy density is:

$$\frac{dU}{dt} = -\frac{1}{\varepsilon}\frac{\partial \varepsilon}{\partial t}U - \frac{\partial P}{\partial x} + c_0\frac{\partial U}{\partial x} = -\frac{1}{\varepsilon}\frac{\partial \varepsilon}{\partial t}U - \frac{\partial P'}{\partial x}, \quad (6)$$

where the compensated Poynting vector P' consists of a local and an advective part (due to the moving frame) [26]. The first term in Eq. 6 is responsible for gain, whereas the second drives the compression of the pulse.

Ignoring the Poynting vector leads to the zero-order solution:

$$U(X,t) = e^{-2\alpha\Omega t \sin(gX)}, \tag{7}$$

where $X = x - \frac{\Omega}{g}t$. Feeding this into the resulting compensated Poynting vector $P' = c_0(\varepsilon(X,t)^{-\frac{1}{2}} - 1)U$ in Eq. 6, we can obtain a corrected expression for the energy density:

$$U(X,t) = \exp\left[-2\alpha\Omega t \sin(gX) - \alpha^2\Omega^2 t^2 \cos^2(gX)\right]. \tag{8}$$

Since the DLG plasmon bands are approximately linear, we can set $c_0 = c_p$ in this closed-form solution, and compare it to our Floquet-Bloch theory for the acoustic plasmons. At the gain point, where the wave grows exponentially with modulation time T_f, frequency Ω, and amplitude α, the two calculations match exactly, as shown in Fig. 2d. As evident from the absence of any frequency dependence in our analytic model, parametric amplification in a luminal medium is completely broadband and its bandwidth is only limited by the extent of the linear dispersion of waves in the medium, which, in the case of DLG, can be made as wide as tens of THz, by reducing the interlayer gap δ_0. This includes the amplification of a DC electric field, which can be compressed and transformed into a narrow pulse via this mechanism.

Fig. 2e demonstrates the total power amplification achieved by our luminal graphene metasurface: initially the unit input power of the wave is predominantly dissipated by the uniform losses, except at the gain-point, so that this first propagation moment is dominated by damping. Once sufficient power is accumulated at the gain-point, the energy fed by the modulation into the plasmon ensures that its propagation is effectively loss-compensated, as in the case of $\alpha = 0.08$, extending its lifetime by orders of magnitude, or even amplified, as in the $\alpha = 0.1$ case.

As the luminal modulation couples the frequency content of the pulse to very high frequency-wavevector harmonics, these will experience the nonlinearity of the bands. In Fig. 3 we use a wider inter-layer gap $\delta_0 = 15$ nm to highlight the effects of dispersion on the pulse profile (a) and its spectral content (b) for different modulation times T_f. At a first stage, since higher frequency components experience a lower phase velocity, the gain-point must shift back to $gX < \frac{\pi}{2}$, where the increase in local phase velocity determined by the modulated Fermi energy compensates for the curvature of the band (Fig. 3, inset). In addition, Fourier components propagating with phase velocity c_p are amplified near the conventional gain-point, resulting in the the pulse becoming skewed ($T_f = 5\tau$). Secondly, for even longer propagation times, the wave will cease to compress, and break into a train of pulses. This is due to the existence of a finite regime of phase velocities:
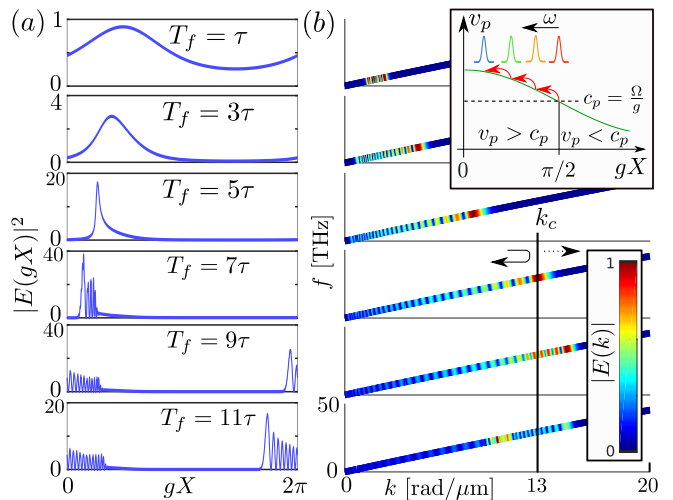

FIG. 3. (a) The onset of dispersion causes a shift of the gain-point due to the slower phase velocity of higher frequency components. In addition, the pulse becomes skewed, due to the superposition of lower frequency components, which are amplified near $gX = \pi/2$, and higher frequency components, which lag behind. For longer modulation times still, the wave breaks into a train of narrow pulses. (b) The spectral content of the pulse is amplified and projected from an input frequency of ≈ 4 THz, to ≈ 30 THz, demonstrating efficient terahertz frequency generation using a modulation frequency of only $\Omega/2\pi = 120$ GHz. High frequency components whose phase velocity is below the instability threshold are not coupled to, hence dispersion stabilizes the system. Here we assumed a wider gap $\delta_0 = 15$ nm to highlight the effect of dispersion, $\alpha = 0.05$, $m = 10^6$ cm^2/(V·s).

$$(1 + 2\alpha)^{-1/2} < v_p/c_p < (1 - 2\alpha)^{-1/2}, \tag{9}$$

within which the interaction between the co-propagating bands is strong enough to make the system unstable [22]. In our setup, the relative phase velocity:

$$\frac{v_p(k)}{c_p} = \left(\frac{\omega(k)}{k}\right)/\left(\frac{\Omega}{g}\right) \simeq \left(\frac{1 - e^{-k\delta_0}}{\delta_0 k}\right)^{1/2} \tag{10}$$

decreases approximately linearly with increasing wavevector [26]. Equating the latter to the lower threshold velocity ratio $v_p(k_c)/c_p = \frac{1}{\sqrt{1+2\alpha}}$, where $\alpha = 0.05$ and expanding the exponential to second order, we get an analytical estimate for the critical wavevector $k_c \approx 13$ rad·μm, beyond which the pulse is no longer strongly coupled to higher harmonics, and its power spectrum is effectively reflected, resulting in beating. Subsequently, the power spectrum oscillates within the extended luminal region, although beating between different space-time harmonics induces fast oscillations which are reminiscent of comb formation in nonlinear optics [52].

In this Letter, we have introduced the concept of luminal metamaterials, realized by inducing a traveling-wave modulation in the refractive index of a material,

whose phase velocity matches that of the waves propagating in it in absence of modulation. We have shown that these dynamical structures act as broadband amplifiers, capable of reinforcing and compressing waves of any frequency, including DC. In addition, we demonstrated the robustness of luminal gratings against significant detuning of the modulation speed, and how the effect can survive even moderate dispersion. We have proposed a realistic setup where this concept could be implemented, consisting of modulated double-layer graphene.

Thanks to its ability to efficiently couple incident electromagnetic waves to frequency harmonics orders of magnitude higher than the input wave, the luminal metamaterial concept suggests a new path towards efficient terahertz generation. Moreover, this scheme constitutes a route towards the compression of graphene plasmons without the need for low doping, thus combining longer plasmon lifetimes with nano-scale confinement. Finally, our setup can achieve loss compensation, and potentially even amplification of plasmons in sufficiently high-quality graphene, holding promises for experimental realizations in the near future.

This concept, which is in principle applicable to any wave phenomenon, could be further generalized by introducing chirping, in analogy with the tuning of the driving field with the energy of the electrons being accelerated in a synchrocyclotron, or it could exploited within narrower frequency bands of strongly dispersive systems.

[1] Amr M Shaltout, Vladimir M Shalaev, and Mark L Brongersma. Spatiotemporal light control with active metasurfaces. *Science*, 364(6441):eaat3100, 2019.

[2] Dimitrios L Sounas and Andrea Alù. Non-reciprocal photonics based on time modulation. *Nature Photonics*, 11(12):774, 2017.

[3] Yakir Hadad, Jason C Soric, and Andrea Alu. Breaking temporal symmetries for emission and absorption. *Proceedings of the National Academy of Sciences*, 113(13):3471–3475, 2016.

[4] Christophe Caloz, Andrea Alù, Sergei Tretyakov, Dimitrios Sounas, Karim Achouri, and Zoé-Lise Deck-Léger. Electromagnetic nonreciprocity. *Phys. Rev. Applied*, 10:047001, Oct 2018.

[5] Da-Wei Wang, Hai-Tao Zhou, Miao-Jun Guo, Jun-Xiang Zhang, Jörg Evers, and Shi-Yao Zhu. Optical diode made from a moving photonic crystal. *Phys. Rev. Lett.*, 110:093901, Feb 2013.

[6] Dimitrios L Sounas, Christophe Caloz, and Andrea Alu. Giant non-reciprocity at the subwavelength scale using angular momentum-biased metamaterials. *Nature communications*, 4:2407, 2013.

[7] Zongfu Yu and Shanhui Fan. Complete optical isolation created by indirect interband photonic transitions. *Nature photonics*, 3(2):91, 2009.

[8] Kejie Fang, Zongfu Yu, and Shanhui Fan. Photonic aharonov-bohm effect based on dynamic modulation. *Phys. Rev. Lett.*, 108:153901, Apr 2012.

[9] Theodoros T Koutserimpas, Andrea Alù, and Romain Fleury. Parametric amplification and bidirectional invisibility in pt-symmetric time-floquet systems. *Physical Review A*, 97(1):013839, 2018.

[10] Nima Chamanara and Christophe Caloz. Linear pulse compansion using co-propagating space-time modulation. *arXiv preprint arXiv:1810.04129*, 2018.

[11] Vincent Ginis, Philippe Tassin, Thomas Koschny, and Costas M Soukoulis. Tunable terahertz frequency comb generation using time-dependent graphene sheets. *Physical Review B*, 91(16):161403, 2015.

[12] Michelle C Sherrott, Philip WC Hon, Katherine T Fountaine, Juan C Garcia, Samuel M Ponti, Victor W Brar, Luke A Sweatlock, and Harry A Atwater. Experimental demonstration of¿ 230 phase modulation in gate-tunable graphene–gold reconfigurable mid-infrared metasurfaces. *Nano letters*, 17(5):3027–3034, 2017.

[13] Qian Lin, Meng Xiao, Luqi Yuan, and Shanhui Fan. Photonic weyl point in a two-dimensional resonator lattice with a synthetic frequency dimension. *Nature communications*, 7:13731, 2016.

[14] Romain Fleury, Alexander B Khanikaev, and Andrea Alu. Floquet topological insulators for sound. *Nature communications*, 7:11744, 2016.

[15] Li He, Zachariah Addison, Jicheng Jin, Eugene J Mele, Steven G Johnson, and Bo Zhen. Floquet chern insulators of light. *arXiv preprint arXiv:1902.08560*, 2019.

[16] Theodoros T Koutserimpas and Romain Fleury. Non-reciprocal gain in non-hermitian time-floquet systems. *Physical review letters*, 120(8):087401, 2018.

[17] Alois Regensburger, Christoph Bersch, Mohammad-Ali Miri, Georgy Onishchukov, Demetrios N Christodoulides, and Ulf Peschel. Parity–time synthetic photonic lattices. *Nature*, 488(7410):167, 2012.

[18] Sanford H Barnes and John E Mann. Voltage sensitive semiconductor capacitor, June 20 1961. US Patent 2,989,671.

[19] John Robinson Pierce. Traveling-wave tubes. *The bell System technical journal*, 29(2):189–250, 1950.

[20] Dimitrios L Sounas, Jason Soric, and Andrea Alu. Broadband passive isolators based on coupled nonlinear resonances. *Nature Electronics*, 1(2):113, 2018.

[21] ES Cassedy and AA Oliner. Dispersion relations in time-space periodic media: Part istable interactions. *Proceedings of the IEEE*, 51(10):1342–1359, 1963.

[22] ES Cassedy. Dispersion relations in time-space periodic

media part iiunstable interactions. *Proceedings of the IEEE*, 55(7):1154–1168, 1967.

[23] Fabio Biancalana, Andreas Amann, Alexander V Uskov, and Eoin P Oreilly. Dynamics of light propagation in spatiotemporal dielectric structures. *Physical Review E*, 75(4):046607, 2007.

[24] Sajjad Taravati, Nima Chamanara, and Christophe Caloz. Nonreciprocal electromagnetic scattering from a periodically space-time modulated slab and application to a quasisonic isolator. *Phys. Rev. B*, 96:165144, Oct 2017.

[25] M. Blaauboer, A. G. Kofman, A. E. Kozhekin, G. Kurizki, D. Lenstra, and A. Lodder. Superluminal optical phase conjugation: Pulse reshaping and instability. *Phys. Rev. A*, 57:4905–4912, Jun 1998.

[26] Supplementary material, including citation [53].

[27] Joshua N. Winn, Shanhui Fan, John D. Joannopoulos, and Erich P. Ippen. Interband transitions in photonic crystals. *Phys. Rev. B*, 59:1551–1554, Jan 1999.

[28] D Correas-Serrano, JS Gomez-Diaz, DL Sounas, Y Hadad, A Alvarez-Melcon, and A Alù. Nonreciprocal graphene devices and antennas based on spatiotemporal modulation. *IEEE Antennas and Wireless Propagation Letters*, 15:1529–1532, 2015.

[29] Tolga Dinc, Mykhailo Tymchenko, Aravind Nagulu, Dimitrios Sounas, Andrea Alu, and Harish Krishnaswamy. Synchronized conductivity modulation to realize broadband lossless magnetic-free non-reciprocity. *Nature communications*, 8(1):795, 2017.

[30] KS Novoselov, A Mishchenko, A Carvalho, and AH Castro Neto. 2d materials and van der waals heterostructures. *Science*, 353(6298):aac9439, 2016.

[31] DN Basov, MM Fogler, and FJ García De Abajo. Polaritons in van der waals materials. *Science*, 354(6309):aag1992, 2016.

[32] Frank HL Koppens, Darrick E Chang, and F Javier García de Abajo. Graphene plasmonics: a platform for strong light–matter interactions. *Nano letters*, 11(8):3370–3377, 2011.

[33] A. Yu. Nikitin, F. Guinea, F. J. Garcia-Vidal, and L. Martin-Moreno. Fields radiated by a nanoemitter in a graphene sheet. *Phys. Rev. B*, 84:195446, Nov 2011.

[34] AN Grigorenko, Marco Polini, and KS Novoselov. Graphene plasmonics. *Nature photonics*, 6(11):749, 2012.

[35] Long Ju, Baisong Geng, Jason Horng, Caglar Girit, Michael Martin, Zhao Hao, Hans A Bechtel, Xiaogan Liang, Alex Zettl, Y Ron Shen, et al. Graphene plasmonics for tunable terahertz metamaterials. *Nature nanotechnology*, 6(10):630, 2011.

[36] Ashkan Vakil and Nader Engheta. Transformation optics using graphene. *Science*, 332(6035):1291–1294, 2011.

[37] Tetiana M Slipchenko, ML Nesterov, Luis Martin-Moreno, and A Yu Nikitin. Analytical solution for the diffraction of an electromagnetic wave by a graphene grating. *Journal of Optics*, 15(11):114008, 2013.

[38] Paloma A Huidobro, Matthias Kraft, Stefan A Maier, and John B Pendry. Graphene as a tunable anisotropic or isotropic plasmonic metasurface. *ACS nano*, 10(5):5499–5506, 2016.

[39] Jean-Marie Poumirol, Peter Q Liu, Tetiana M Slipchenko, Alexey Y Nikitin, Luis Martin-Moreno, Jérôme Faist, and Alexey B Kuzmenko. Electrically controlled terahertz magneto-optical phenomena in continuous and patterned graphene. *Nature communications*, 8:14626, 2017.

[40] Chi-Fan Chen, Cheol-Hwan Park, Bryan W Boudouris, Jason Horng, Baisong Geng, Caglar Girit, Alex Zettl, Michael F Crommie, Rachel A Segalman, Steven G Louie, et al. Controlling inelastic light scattering quantum pathways in graphene. *Nature*, 471(7340):617, 2011.

[41] Dmitri K Efetov and Philip Kim. Controlling electron-phonon interactions in graphene at ultrahigh carrier densities. *Physical review letters*, 105(25):256805, 2010.

[42] Wei Li, Bigeng Chen, Chao Meng, Wei Fang, Yao Xiao, Xiyuan Li, Zhifang Hu, Yingxin Xu, Limin Tong, Hongqing Wang, et al. Ultrafast all-optical graphene modulator. *Nano letters*, 14(2):955–959, 2014.

[43] Luca Banszerus, Michael Schmitz, Stephan Engels, Jan Dauber, Martin Oellers, Federica Haupt, Kenji Watanabe, Takashi Taniguchi, Bernd Beschoten, and Christoph Stampfer. Ultrahigh-mobility graphene devices from chemical vapor deposition on reusable copper. *Science advances*, 1(6):e1500222, 2015.

[44] Tiago A Morgado and Mário G Silveirinha. Negative landau damping in bilayer graphene. *Physical review letters*, 119(13):133901, 2017.

[45] Tobias Wenger, Giovanni Viola, Jari Kinaret, Mikael Fogelström, and Philippe Tassin. Current-controlled light scattering and asymmetric plasmon propagation in graphene. *Phys. Rev. B*, 97:085419, Feb 2018.

[46] Josh Wilson, Fadil Santosa, Misun Min, and Tony Low. Temporal control of graphene plasmons. *Phys. Rev. B*, 98:081411, Aug 2018.

[47] Zhiyuan Sun, DN Basov, and MM Fogler. Adiabatic amplification of plasmons and demons in 2d systems. *Physical review letters*, 117(7):076805, 2016.

[48] Ido Kaminer, Yaniv Tenenbaum Katan, Hrvoje Buljan, Yichen Shen, Ognjen Ilic, Josué J López, Liang Jie Wong, John D Joannopoulos, and Marin Soljačić. Efficient plasmonic emission by the quantum čerenkov effect from hot carriers in graphene. *Nature communications*, 7:11880, 2016.

[49] Paulo André Dias Gonçalves and Nuno MR Peres. *An introduction to graphene plasmonics*. World Scientific, 2016.

[50] David Alcaraz Iranzo, Sébastien Nanot, Eduardo JC Dias, Itai Epstein, Cheng Peng, Dmitri K Efetov, Mark B Lundeberg, Romain Parret, Johann Osmond, Jin-Yong Hong, et al. Probing the ultimate plasmon confinement limits with a van der waals heterostructure. *Science*, 360(6386):291–295, 2018.

[51] Eduardo J. C. Dias, David Alcaraz Iranzo, P. A. D. Gonçalves, Yaser Hajati, Yuliy V. Bludov, Antti-Pekka Jauho, N. Asger Mortensen, Frank H. L. Koppens, and N. M. R. Peres. Probing nonlocal effects in metals with graphene plasmons. *Phys. Rev. B*, 97:245405, Jun 2018.

[52] PL Knight and A Miller. *Optical solitons: theory and experiment*, volume 10. Cambridge University Press, 1992.

[53] T Stauber, NMR Peres, and F Guinea. Electronic transport in graphene: A semiclassical approach including midgap states. *Physical Review B*, 76(20):205423, 2007.